

SESSION XIII: Charge-Coupled Devices and Applications

THPM 13.2: Diagnostic Analysis of the Charge Transfer in CCDs

Hans Wallinga and Hans L. M. van Ruyven

Twente University of Technology

Enschede, Netherlands

AFTER THE INTRODUCTION of the CCD concept several researchers proposed models for the transfer process in MOS transistor structures¹⁻⁵. Experimental verification of those models was however difficult, particularly when short time intervals (< 100 ns) were involved. The project to be described involves a small signal method^{6,7} and uses the CCD as a tool to obtain experimental data about the single charge transfer process. Experimental results will be compared with predictions based on the charge control model². The experiments were performed on a 7-bit 4-phase P-channel device with two level aluminum gates; Figure 1. The device was designed for analysis purposes rather than for optimum CCD operation.

Figure 2 shows the applied clock wave forms. They are chosen such that the charge transfers $F1 \rightarrow F2$ and $F3 \rightarrow F4$ are complete. Furthermore the conditions provide intentionally for a large transfer inefficiency of the transfers $F2 \rightarrow F3$ and $F4 \rightarrow F1$, when the background charge packet exceeds the capacity of the potential well below $F3$ during the overlap of $F2$ and $F3$. During the time interval $t1$ to $t4$, $F2$ declines and the remaining charge below $F2$ is transferred. With the help of Figure 2 it will be clear that at $t3$ the unidirectional slope of the potential below $F2$ is disturbed and from then on also backward transfer towards $F1$ will occur. It is assumed that the remaining charge $Q(t_{eff})$ below $F2$ at time $t3$, completely distributes in equal parts between $F1$ and $F3$; thus $\frac{1}{2} Q(t_{eff})$ will remain below $F1$ and contributes to the charge transfer inefficiency.

It was assumed that this amount of charge was easy to vary by controlling t_{eff} , which is in turn a function of the falltime of $F2$ and the background charge packet Q . For the charge control

model, an expression for the remaining charge $Q(t_{eff})$ had been derived²: equation (1) in Figure 3. As the boundary conditions require a zero charge concentration at the sink boundary, the transfer was allowed to start at $t2$; the time for which the bottom of the potential well below $F2$ equals the filled level below $F3$. Furthermore it was assumed that the charge transfer during t_{eff} is caused by self-induced drift and diffusion. The influence of surface states on the transfer inefficiency is neglected.

The expression for the small signal transfer inefficiency parameter ϵ is shown as equation (2) in Figure 3. The data computed from equation (2) are plotted in Figures 4 and 6.

The experiments consisted of the input - output phase shift measurements of the complete CCD, using a small sinusoidal input signal ($V_{eff} = 50$ mV, $f = 10$ kHz) superimposed on a constant background dc signal. Clock frequency was 250 kHz.

As derived earlier⁶, the charge transfer inefficiency causes an extra phase shift. For a two-transfer-per-cell arrangement their

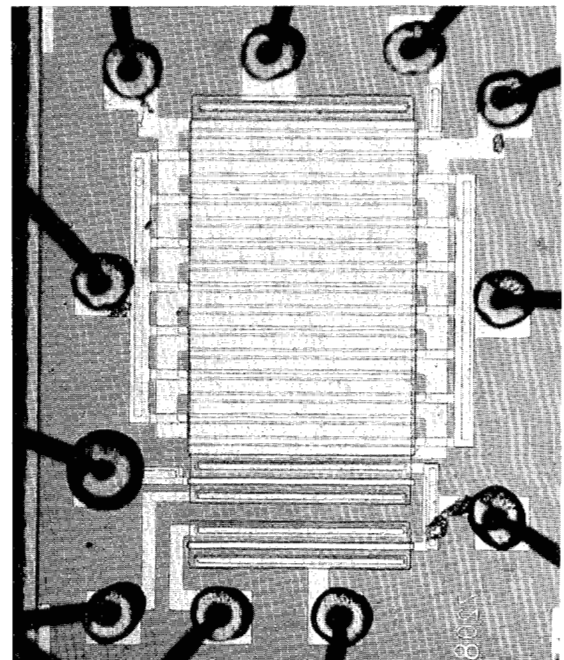


FIGURE 1—View of 7-bit, 4-phase, P-channel CCD chip*. Epilayer concentration $N_D = 2.10^{15} \text{ cm}^{-3}$; oxide thickness $d_1 = 0.20 \text{ } \mu\text{m}$, $d_2 = 0.31 \text{ } \mu\text{m}$; gatelength $L_1 = 19 \text{ } \mu\text{m}$, $L_2 = 23 \text{ } \mu\text{m}$; gatewidth $W = 400 \text{ } \mu\text{m}$; threshold voltage $V_{T1} = 2.0 \text{ V}$, and $V_{T2} = -3.3 \text{ V}$.

¹ Kim, C. K., and Lenzinger, M., "Charge Transfer in Charge-Coupled Devices", *J. Appl. Phys.*, p. 3586-3594; Aug., 1971.

² Lee, H. S., and Heller, L. G., "Charge-Control Method of Charge-Coupled Device Transfer Analysis", *IEEE Trans. Electron Devices*, p. 1270-1279; Dec., 1972.

³ Carnes, J. E., Kosonocky, W. F. and Ramberg, E. G., "Free Charge Transfer in Charge-Coupled Devices", *IEEE Trans. Electron Devices*, p. 798-808; June, 1972.

⁴ Berglund, C. N. and Thornber, K. K., "A Fundamental Comparison of Incomplete Charge Transfer in Charge Transfer Devices", *B.S.T.J.*, p. 147-182; Feb., 1972.

⁵ Engeler, W. E., Tiemann, J. J., and Baertsch, R. D., "Surface-Charge Transport in a Multi-Element Charge-Transfer Structure", *J. Appl. Phys.*, p. 2277-2285; May, 1972.

⁶ Joyce, W. B. and Bertram, W. J., "Linearized Dispersion Relation and Green's Function for Discrete-Charge-Transfer Devices with Incomplete Transfer", *B.S.T.J.*, p. 1741-1759; July-Aug., 1971.

⁷ Berglund, C. N. and Thornber, K. K., "Incomplete Transfer in Charge-Transfer Devices", *IEEE J. Solid-State Circuits*, p. 108-116; April, 1973.

treatment requires a modification, leading to the following expression for the phase shift ϕ_1 per cell:

$$\phi_1 = \text{arctg} \left(\frac{(1 - \epsilon^2) \sin \omega}{(1 + \epsilon^2) \cos \omega - 2 \epsilon} \right) \quad (3)$$

where ω denotes 2π times the ratio of the signal frequency and clock frequency.

Experimental data are plotted in Figures 5 and 6.

The proposed experimental analysis offers a fast and easy instrument measurement method for the analysis of the charge transfer process. Advantage is taken of the sensitive small signal method. Both the background charge packet and the effective transfer time are independent variables, while unlike the experiments with variable clock frequencies, other circumstances are unchanged. Figure 6 shows that a more accurate model is required.

Acknowledgments

We wish to acknowledge O. W. Memelink for stimulating discussions and criticism, and the members of the technology group of our laboratory for the preparation of the devices.

*P208.

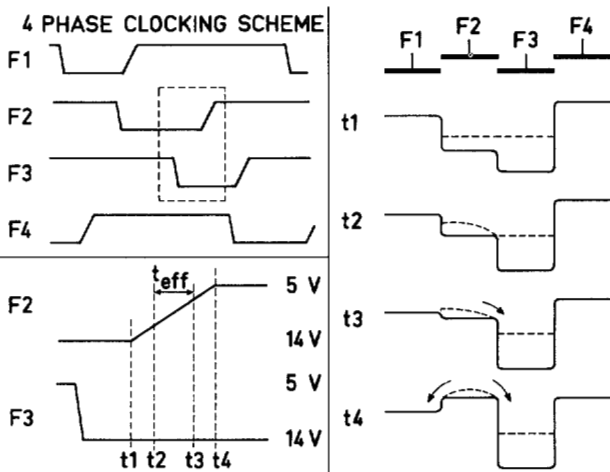


FIGURE 2—Four-phase clocking scheme and surface potential distribution for one cell of CCD at four characteristic times.

$$Q(t_{\text{eff}}) = \frac{Q(o) \exp(-K t_{\text{eff}}/t_{\text{tr}})}{1 + (Q(o) \pi^2 / 8 C K) (1 - \exp(-K t_{\text{eff}}/t_{\text{tr}}))} \quad (1)$$

$$\epsilon = \frac{d \frac{1}{2} Q(t_{\text{eff}})}{d Q} = \frac{1}{4} (F(t_{\text{eff}}))^2 \exp(K t_{\text{eff}}/t_{\text{tr}}) \quad (2)$$

where $F(t_{\text{eff}}) = \frac{Q(t_{\text{eff}})}{Q(o)}$, $\frac{dQ(o)}{dQ} = \frac{1}{2}$

$K = \pi^2 D_p / 4 \mu_p \approx 0.062 \text{ V}$ $Q =$ background charge packet
 $t_{\text{tr}} = L_1^2 / \mu_p \approx 2.6 \cdot 10^{-8} \text{ Vs}$ $Q(o) =$ charge packet below F_2 at t_1
 $t_{\text{eff}} =$ effective transfertime $Q(t_{\text{eff}}) =$ remaining packet below F_2 at t_3
 $C =$ inversion layer capacity

FIGURE 3—The small-signal charge-transfer inefficiency ϵ , derived from the charge control model.

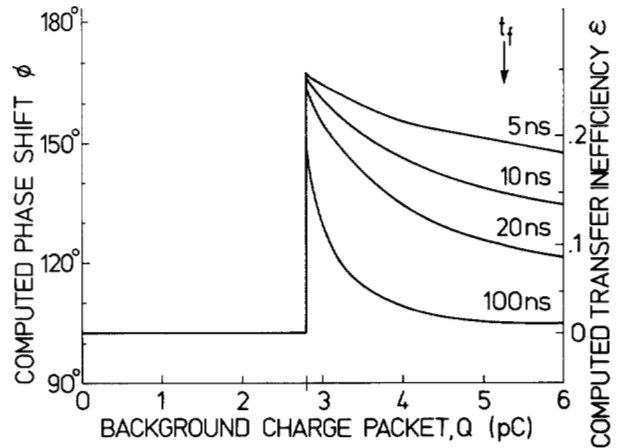


FIGURE 4—Computed transfer inefficiency ϵ and corresponding phaseshift ϕ of the CCD with the falltime t_f of F_2 as a parameter.

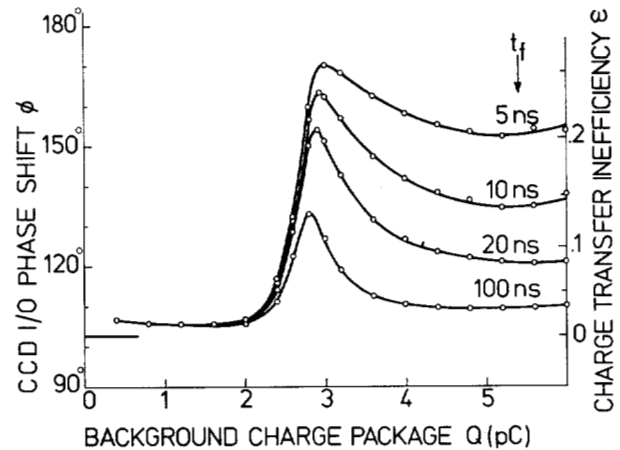


FIGURE 5—Measured phaseshift between input and output of the CCD and corresponding transfer inefficiency ϵ , with the falltime t_f of F_2 as a parameter.

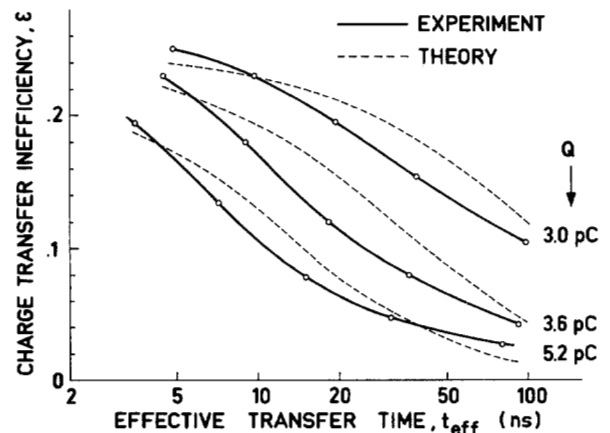


FIGURE 6—Experimental and theoretical values of ϵ , as a function of t_{eff} , with the background charge packet Q as a parameter.